Coupling finite volume and nonstandard finite difference schemes for a singularly perturbed Schrödinger equation

A. A. Aderogba, M. Chapwanya*, J. Djoko Kamdem, J. M.-S. Lubuma

Department of Mathematics & Applied Mathematics, University of Pretoria, Pretoria, South Africa

Abstract

The Schrödinger equation is a model for many physical processes in quantum physics. It is a singularly perturbed differential equation where the presence of the small reduced Planck's constant makes the classical numerical methods very costly and inefficient. We design two new schemes. The first scheme is the nonstandard finite volume method, whereby the perturbation term is approximated by nonstandard technique, the potential is approximated by its mean value on the cell and the complex dependent boundary conditions are handled by exact schemes. In the second scheme, the deficiency of classical schemes is corrected by the inner expansion in the boundary layer region. Numerical simulations supporting the performance of the schemes are presented.

Keywords: Schrödinger equation; oscillatory preserving schemes, finite volume method; nonstandard finite difference method.
2010 AMS Subject Classification: 65M06; 65M08; 97N40

1 Introduction

The Schrödinger differential model

$$\begin{cases} -\varepsilon^2 u''(x) - q(x)u(x) = 0, \quad x \in (a,b), \\ \varepsilon u'(a) + \imath p(a)u(a) = 2\imath p(a), \\ \varepsilon u'(b) - \imath p(b)u(b) = 0, \end{cases} \tag{1.1}$$

where $\imath = \sqrt{-1}$, $q(x) = E - V(x) > 0$ is the potential with $p(x) = \sqrt{q(x)}$ and $\varepsilon \ll 1$, falls into the class of equations known as singularly perturbed equations and is characterized by strongly oscillatory solutions. This behaviour requires that, for any difference scheme to accurately approximate its solution, the wavelength, $\lambda = \min_x \left(2\pi\varepsilon/\sqrt{q(x)}\right)$, must always be greater than the

*Corresponding author. m.chapwanya@up.ac.za; Tel.: +27 12 420 2837; Fax.: +27 12 420 3893

discrete space width, where the minimum is taken over space. This makes its numerical approximation computationally costly. In particular, in [3] it was pointed out that most numerical schemes require at least 10 grid points per oscillation.

Physical processes modeled by the Schrödinger equation find applications in both industrial and domestic purposes such as design of semiconductor appliances in quantum and plasma physics, resonant tunneling diodes, microwaves, etc. Therefore, a lot of research on the solution of equation (1.1) has been done based on standard finite difference (both classical, adaptive mesh and finite volume), finite element and WKB methods, see for example [3] and the literature therein. The authors in [9] solved the Schrödinger equation on a non-uniform mesh using a finite difference method. They observed that the method had better convergence properties compared to the classical finite difference or finite element methods. A recent investigation on designing faster convergent schemes is found in [10] where the Schrödinger-Poisson equation arising from models in resonant tunneling diode was investigated. The author employed the Gummel method to achieve faster convergence. The challenge of high computational cost was addressed by employing adaptive mesh size in which case the mesh will only be refined at the resonance regions. With the same focus on reducing the computational cost, the authors in [11] discussed a method which was later rigorously analyzed in [12]. They employed the finite element method with the basis elements coming from the WKB approximation. Most recently on this trend, the authors in [3] claimed that the high computational cost of classical methods is due to the requirement that the space width be smaller compared to the wavelength of the solution. This idea forms the basis of our current work.

In this paper, we design two robust finite volume based schemes that are capable of reducing the computational cost associated with most classical schemes. The first scheme is based on the non-standard finite difference (NSFD) method which originated from the work of Mickens, [13, 14]. We highlight that NSFD schemes have been efficient in tackling the deficiency of classical finite difference schemes for the approximation of solutions of several differential equation models, see for example [16, 17, 18, 19, 20] and the literature therein. Here we also highlight the work [1, 6], which differs from the approach adopted here in the sense that their NSFD schemes are derived by adopting a Green's function approach which offers a good platform to develop nontrivial schemes for a range of reaction diffusion equations. For more on the application and earlier developments on the NSFD the reader can consult [14, 15]. The second non classical finite volume (NCFV) scheme, motivated by asymptotic approximations, is derived following the work [21, 22].

The remaining part of this article is as follows. We begin by formulating the asymptotic approximate solutions in Section 2. Section 3 is devoted to the discussion of the classical finite volume methods followed by Section 4 where we develop the idea of NSFD schemes. Derivation of the NCFV scheme is the focus of Section 5. In Section 6 we design a non-standard finite volume (NSFV) scheme followed by Section 7 where some numerical experiments on the performance of the schemes are presented. We finish with Section 8 where we summarize our observations.

2 Approximate analytical solution

In this section, we carry out the perturbation analysis on problem (1.1). This approach enables us to show that the Schrödinger equation is a singularly perturbed equation and hence identify the stiffness which make the classical schemes less efficient. The regular perturbation is based on the

ansatz

$$u = \sum_{k=0}^{\infty} \varepsilon^k u_k, \tag{2.1}$$

where the perturbation parameter is ε. This leads to the outer expansion of equation $(1.1)_1$. Substituting equation (2.1) into (1.1) and equating the powers of ε leads to

$$\begin{cases} u_0(x) = u_1(x) = 0, \\ -u''_{k-2}(x) - q(x)u_k(x) = 0, \quad k > 0. \end{cases} \tag{2.2}$$

At $x = a$ we have that

$$\begin{cases} u_0(a) = 2, \\ u'_{k-1}(a) + \imath p(a)u_k(a) = 0, \quad k > 0, \end{cases} \tag{2.3}$$

and at $x = b$ we have

$$\begin{cases} u_0(b) = 0, \\ u'_{k-1}(b) - \imath p(b)u_k(b) = 0, \quad k > 0. \end{cases} \tag{2.4}$$

From equations (2.2), (2.3) and (2.4) it is observed that at leading order, u_0 does not agree with the boundary condition $u_0(a) = 2$ though it satisfies $u_0(b) = 0$. This suggests there is a boundary layer at $x = a$. In order to resolve this, and following [21], we carry out an inner expansion at $x = a$ and this motivates the development of the NCFV scheme in Section 5. However, for better accuracy here we seek for the solution to equation $(1.1)_1$ using the WKB method to get an explicit solution [7],

$$\theta(x) \sim -q(x)^{-\frac{1}{4}} \left[\alpha_0 \exp\left(-\imath \frac{1}{\varepsilon} \int^x \sqrt{q(s)} ds \right) + \beta_0 \exp\left(\imath \frac{1}{\varepsilon} \int^x \sqrt{q(s)} ds \right) \right], \tag{2.5}$$

where the values of α_0 and β_0 are found via the boundary conditions. Looking ahead, this solution will only be used as a corrector at the boundary layer in the development of the NCFV scheme.

Remark 2.1 *The above derivation differs from the literature since the authors in [21] obtained the correctors by expanding the solution and the coefficients in terms of the auxiliary variable $\bar{x} = x/\varepsilon$. We believe that our approach is less computationally extensive, and yet produce reliable results, see the numerical section.*

3 Classical finite volume scheme

In this work we will employ the finite volume discretization on a uniform mesh: $x_j = jh$, where $j = 0, 1, 2, \cdots m$, are the nodal points and $h = (b-a)/m$ is the grid size and m is the total number of cells. Thus u_j are the nodal values and obviously, x_{-1} and x_{m+1} are ghost points whose values are approximated using the boundary conditions. In the finite volume context, the values of the unknowns are computed not at the nodal points but at the interfaces $x_{j\pm\frac{1}{2}} = x_j \pm h/2$.

We develop the idea of finite volume method for $(1.1)_1$ by multiplying the equation with the step function $\chi_{(x_{j-\frac{1}{2}},x_{j+\frac{1}{2}})}$ and integrate over the entire space Ω to get

$$-\varepsilon^2 u'(x)\Big|_{x_{j-\frac{1}{2}}}^{x_{j+\frac{1}{2}}} - \int_{x_{j-\frac{1}{2}}}^{x_{j+\frac{1}{2}}} q(x)u dx = 0. \tag{3.1}$$

The solution u and its derivative u' are interpolated as in [22], i.e.,

$$u(x) \approx u_h(x) = \sum_{j=1}^{m} u_j \chi_{(x_{j-\frac{1}{2}},x_{j+\frac{1}{2}})}(x),$$

and

$$\begin{aligned} u'(x) \approx \nabla_h u_h &= \sum_{j=0}^{m} \frac{u_{j+1}-u_j}{h}\chi_{(x_j,x_{j+1})}(x), \qquad (3.2)\\ &= \frac{u_1-u_0}{h}\chi_{[x_0,x_1)}(x) + \frac{u_{m+1}-u_m}{h}\chi_{(x_m,x_{m+1}]}(x) + \sum_{j=1}^{m-1}\frac{u_{j+1}-u_j}{h}\chi_{(x_j,x_{j+1})}(x). \end{aligned}$$

With this in mind, equation (3.1) can be written as

$$-\varepsilon^2 \nabla_h u_h\Big|_{x_{j-\frac{1}{2}}}^{x_{j+\frac{1}{2}}} - u_j \int_{x_{j-\frac{1}{2}}}^{x_{j+\frac{1}{2}}} q(x)dx = 0. \tag{3.3}$$

This implies that for $j = 1, 2, 3, \cdots, m-1$, the classical finite volume discretization of the Schrödinger equation (1.1) is given by

$$-\varepsilon^2 \frac{u_{j-1}-2u_j+u_{j+1}}{h^2} - \frac{u_j}{h}\int_{x_{j-\frac{1}{2}}}^{x_{j+\frac{1}{2}}} q(x)dx = 0. \tag{3.4}$$

Notice that equation (3.4) can simply be written as

$$\rho_{j-1}u_{j-1} + \rho_j u_j + \rho_{j+1}u_{j+1} = b_j, \tag{3.5}$$

where the right hand side coefficients b_j are all zero except for b_1 which will be determined through the ghost values. The coefficients are

$$\rho_{j-1} = -\frac{\varepsilon^2}{h^2}, \quad \rho_j = \frac{2\varepsilon^2}{h^2} - \bar{q}_j, \quad \rho_{j+1} = -\frac{\varepsilon^2}{h^2}, \tag{3.6}$$

where

$$\bar{q}_j = \frac{1}{h}\int_{x_{j-\frac{1}{2}}}^{x_{j+\frac{1}{2}}} q(x)dx,$$

are values of a tri-diagonal matrix ρ, for $j = 1, 2, \cdots, m-1$. Using $(1.1)_{2-3}$, the discrete ghost values are obtained via the following finite volume approximations at the boundaries

$$\varepsilon\frac{u_{0+\frac{1}{2}} - u_{0-\frac{1}{2}}}{h} + \imath p(a)u_0 = 2\imath p(a), \tag{3.7}$$

$$\varepsilon\frac{u_{m+\frac{1}{2}} - u_{m-\frac{1}{2}}}{h} - \imath p(b)u_m = 0, \tag{3.8}$$

where $u_{m\pm\frac{1}{2}} = (u_m + u_{m\pm1})/2$. We note that equation (3.5) is a tri-diagonal linear system which can be solved by classical iterative or direct methods.

4 Non-standard finite difference scheme

In this section, we follow [14, 18] and outline the main steps in designing the NSFD scheme for a linear second order equation

$$-\varepsilon^2 u'' - q(x)u = 0, \tag{4.1}$$

where $\varepsilon \ll 1$. We begin by assuming that the function $q(x)$ is a constant and given by $\tilde{q}$. In this case of constant $\tilde{q}$, the exact scheme of (4.1) is given in [14] by

$$\begin{vmatrix} u_j & e^{\imath\lambda hj} & e^{-\imath\lambda hj} \\ u_{j+1} & e^{\imath\lambda h(j+1)} & e^{-\imath\lambda h(j+1)} \\ u_{j+2} & e^{\imath\lambda h(j+2)} & e^{-\imath\lambda h(j+2)} \end{vmatrix} = 0, \tag{4.2}$$

which is equivalent to

$$-\varepsilon^2 \frac{u_{j+1} - 2u_j + u_{j-1}}{\phi^2} - \tilde{q}u_j = 0, \tag{4.3}$$

where

$$\phi = \frac{2\varepsilon}{\sqrt{\tilde{q}}} \sin\left(\frac{\sqrt{\tilde{q}}}{2\varepsilon}h\right).$$

A possible generalization for the variable coefficient differential equation is

$$-\varepsilon^2 \frac{u_{j+1} - 2u_j + u_{j-1}}{\phi_j^2} - q_j u_j = 0, \tag{4.4}$$

where $q_j = q(x_j)$ and

$$\phi_j = \frac{2\varepsilon}{\sqrt{q_j}} \sin\left(\frac{\sqrt{q_j}}{2\varepsilon}h\right).$$

For better qualitative properties, [18] introduced

$$q(x_j) \approx \bar{q}_j = \frac{q_{j-1} + q_j + q_{j+1}}{3}, \tag{4.5}$$

so that

$$\phi_j = \frac{2\varepsilon}{\sqrt{\bar{q}_j}} \sin\left(\frac{\sqrt{\bar{q}_j}}{2\varepsilon}h\right). \tag{4.6}$$

It has been shown that the equation (1.1) when solved subject to Dirichlet boundary condition such that $u(0), u(1) \geq 0$ satisfies the maximum principle and that the schemes (4.3) and (4.4) with (4.6) are qualitatively stable with respect to this property, [18]. For the rest of the paper, scheme (4.4) together with (4.5) and (4.6) will be referred to as the NSFD scheme for the Schrödinger equation $(1.1)_1$.

5 Non classical finite volume scheme

The solution θ in equation (2.5) is enough to correct any shortcomings $x = a$ when combined with the outer expansion without affecting the behavior of the solution at $x = b$. Here, the proposed scheme will follow a perturbation in the solution of the form

$$\tilde{u} = u_h + \lambda\theta, \tag{5.1}$$

where $\lambda \in \mathbb{R}$ is unknown and will be determined along with the variable of interest. Now, the boundary condition will be such that

$$\begin{cases} \varepsilon u'(a) + \lambda\theta_x(a) + \imath p(a)u(a) + \imath p(a)\lambda\theta(a) = 2\imath p(a), \\ \varepsilon u'(b) + \lambda\theta_x(b) = \imath p(b)u(b) + \imath p(b)\lambda\theta(b). \end{cases} \tag{5.2}$$

The introduction of λ increases the number of unknowns without increasing the number of equations. Therefore, we need one more equation for uniqueness. First we will multiply the Schrödinger equation by the function $\theta\chi[0, x_{1+\frac{1}{2}}]$ and integrate over (a, b). The idea here is to correct the stiffness at the boundary $x = a$, see the discussion in Section 2 and the reference [21]. We have

$$-\varepsilon^2\nabla_h u_h\theta\Big|_0^{x_{1+\frac{1}{2}}} + \varepsilon^2\int_0^{x_{1+\frac{1}{2}}} \nabla_h u_h\theta_x dx - \int_0^{x_{1+\frac{1}{2}}} \theta q(x)dx = 0, \tag{5.3}$$

which we write in the form

$$\sigma_0\lambda + \sigma_1 u_1 + \sigma_2 u_2 = 0, \tag{5.4}$$

where, on employing interpolation functions in Section 3, we have

$$\begin{aligned} \sigma_0 &= \frac{\varepsilon^2}{h}\theta(x_1)\left(\frac{\theta'(a)h + \imath p(a)\theta(a)h}{\alpha\varepsilon}\right), \\ \sigma_1 &= \frac{\varepsilon^2}{h}\left(\theta(x_{1+\frac{1}{2}}) + \theta(x_1)\frac{\alpha\varepsilon + 1 + \imath p(a)h/(2\varepsilon)}{\alpha\varepsilon}\right) - \int_0^{x_{1+\frac{1}{2}}} q(x)\theta dx, \\ \sigma_2 &= -\frac{\varepsilon^2}{h}\Big(\theta(x_{1+\frac{1}{2}}) - 2\theta(x_2) + \theta(x_1)\Big) - \int_{x_{1+\frac{1}{2}}}^{x_{2+\frac{1}{2}}} q(x)\theta dx, \end{aligned}$$

with

$$\alpha = \imath p(a)h/(2\varepsilon) - 1.$$

Substituting equation (5.1) into (1.1) and integrating over each cell, bearing in mind equation (3.3) and the boundary conditions (5.2), we have

$$\sigma_{j-1}u_{j-1} + \sigma_j u_j + \sigma_{j+1}u_{j+1} = b_j, \tag{5.5}$$

where $b_1 = \dfrac{2\imath p(a)h\varepsilon^2}{h[\imath p(a)h/(2\varepsilon) - 1]\varepsilon}$ and $b_j = 0$ for $j = 2, \cdots, m$. On simplifying, the coefficients in (5.5) remain the same as in the classical scheme except for the following

$$\begin{aligned} \sigma_0 &= -\frac{\varepsilon^2}{h}\left(\frac{h}{\varepsilon}\theta'(0) + \frac{h}{\varepsilon}\theta(0)\right), \\ \sigma_1 &= \frac{\varepsilon^2}{h}\left(2 + \frac{1 + \imath p(a)h/(2\varepsilon)}{\imath p(a)h/(2\varepsilon) - 1}\right), \\ \sigma_2 &= -\frac{\varepsilon^2}{h}. \end{aligned} \tag{5.6}$$

Remark 5.1 *The Scheme* (5.6) *gives the classical finite volume scheme when* $\lambda = 0$ *otherwise NCFV. In addition, our usage of the WKB approximation here is not the same as used, for example, in [3, 11, 12].*

6 Non-standard finite volume scheme

The non-standard finite volume scheme derived here is based on the classical finite volume scheme in Section 3, and the non-standard finite difference scheme derived in Section 4. Thus merging the ideas developed in (3.4), (4.4) and (4.6), we have the non-standard finite volume (NSFV) scheme

$$-\varepsilon^2 \frac{u_{j-1} - 2u_j + u_{j+1}}{\tilde{\phi}_j^2} - \bar{q}_j u_j = 0, \tag{6.1}$$

where the denominator function is given by

$$\tilde{\phi}_j = \frac{2\varepsilon}{\sqrt{\bar{q}_j}} \sin\left(\frac{\sqrt{\bar{q}_j}}{2\varepsilon} h\right),$$

and

$$\bar{q}_j = \frac{1}{h} \int_{x_{j-\frac{1}{2}}}^{x_{j+\frac{1}{2}}} q(x) dx,$$

is the mean-value of $q(x)$ on $[x_{j-\frac{1}{2}}, x_{j+\frac{1}{2}}]$. We note that scheme (6.1), after eliminating ghost points, will result in a linear system of algebraic equations of the form $\rho \mathbf{u} = \mathbf{b}$. Here ρ is a tri-diagonal matrix with entries

$$\rho_{j-1} = \frac{\varepsilon^2}{\tilde{\phi}_{j-1}^2}, \quad \rho_j = -\frac{2\varepsilon^2}{\tilde{\phi}_j^2} + \tilde{q}_j, \quad \rho_{j+1} = \frac{\varepsilon^2}{\tilde{\phi}_{j+1}^2}. \tag{6.2}$$

Remark 6.1 *The elements of the coefficient matrix above differ significantly from those given in equation* (3.6)*. The distinction which arises from the difference in the denominator of equations* (3.4) *and* (6.1) *also accounts for better stability property known with the nonstandard scheme. In addition, we are able to include less regular coefficients.*

We handle the boundary ghost points by designing separate non standard approximation for these equations, an idea that was also used in [4]. At $x = a$ we have,

$$u' + \frac{\imath p(a)}{\varepsilon} u = \frac{2\imath p(a)}{\varepsilon}, \tag{6.3}$$

which has an exact scheme, [14],

$$\varepsilon \frac{u_j - u_{j-1}}{\phi_a(h)} + \imath p(a) u_{j-1} = 2\imath p(a), \tag{6.4}$$

where

$$\phi_a(h) = \frac{1 - \exp\left(-\frac{\imath p(a)}{\varepsilon} h\right)}{\imath p(a)/\varepsilon}.$$

Inserting $j = 0$, we get an approximation for the ghost value u_{-1}. Similarly, at $x = b$ we follow the same idea to get

$$\varepsilon \frac{u_{m+1} - u_m}{\phi_b(h)} = \imath p(b) u_m, \tag{6.5}$$

where

$$\phi_b(h) = \frac{\exp\left(\frac{\imath p(b)h}{\varepsilon}\right) - 1}{\imath p(b)/\varepsilon}.$$

The ghost values u_{-1} and u_{m+1} are eliminated using equations (6.4) and (6.5), respectively. We highlight that using the exact schemes (6.4) and (6.5), where no truncation error arises, should overcome the difficulty caused by classical numerical methods applied to complex boundary conditions $(1.1)_{2-3}$.

7 Numerical Experiments

In this section we present numerical experiments to compare the performance of the classical finite volume scheme (CFV) (3.4)–(3.8), the derived non-classical finite volume scheme (5.6) and the derived non-standard finite volume scheme (6.1). Their efficiency are illustrated via three examples. In the first example, a simplified differential equation with constant potential $q(x) = 1$ is solved on $x \in [0, 1]$ with Dirichlet boundary conditions. The second and third examples consider numerical solution of the Schrödinger equation subject to a continuous and discontinuous potential function $q(x)$, respectively.

Example 1 *Consider*

$$\begin{cases} -\varepsilon^2 u''(x) - u(x) = 0, \;\; x \in (0, 1), \\ u(0) = 1, \quad u(1) = 0. \end{cases} \tag{7.1}$$

The exact solution to (1) is

$$u(x) = \frac{\sin((1-x)/\varepsilon)}{\sin(1/\varepsilon)}.$$

The numerical simulations are presented in Fig. 1 with the maximum error calculations given in Table 1. In the figure, the solid lines represent the exact solution while the dots represent the computed numerical solution. We note that for $q(x) = 1$, the non-standard finite volume scheme (6.1) is exact and this is supported by the solution in Fig. 1(a) and error calculation in Table 1. On the other hand, the distorted solution using a classical finite volume scheme (3.4) is evident in Fig. 1(b) and the corresponding large error in Table 1.

Example 2 *Consider*

$$\begin{cases} -\varepsilon^2 u''(x) - q(x)u(x) = 0, \;\; x \in (0, 1), \\ \varepsilon u'(0) + ip(0)u(0) = 2ip(0), \\ \varepsilon u'(1) - ip(1)u(1) = 0, \end{cases} \tag{7.2}$$

with the potential function $q(x) = \left(x + \frac{1}{2}\right)^2$, $x \in [0, 1]$.

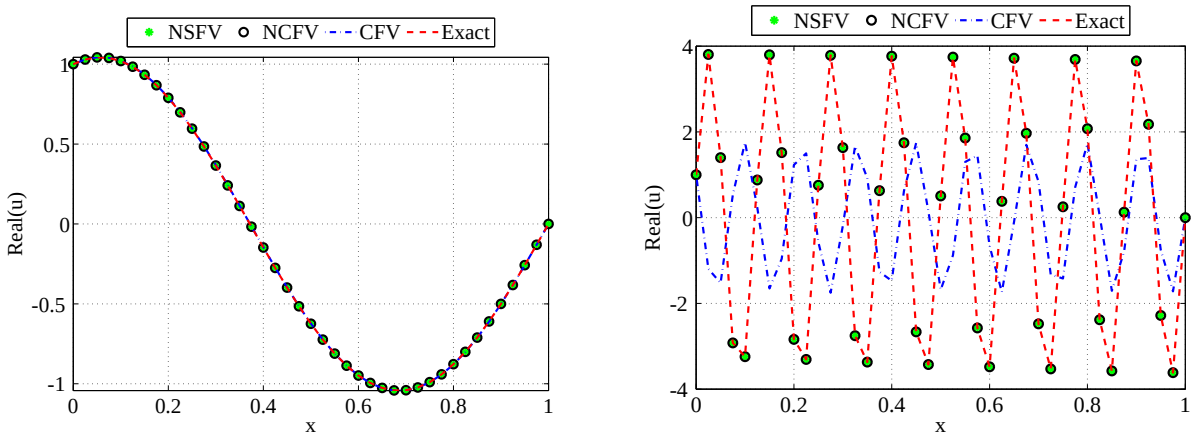

(a) $\varepsilon = 0.2$. (b) $\varepsilon = 0.02$.

Figure 1: A comparison of the classical, non-classical and the non-standard finite volume schemes for $m = 40$.

Grid points	L_∞ Norm error					
	$\varepsilon = 0.02$			$\varepsilon = 0.002$		
	CFV	NSFV $\times 10^{12}$	NCFV$\times 10^{16}$	CFV	NSFV $\times 10^{12}$	NCFV$\times 10^{16}$
16	3.8088	0.2087	2.2204	2.1314	1.3989	4.4409
32	4.7626	0.0773	8.8817	2.1378	6.6613	4.4409
64	4.9046	0.0315	13.322	2.1378	1.4433	4.4409
128	19.6432	0.0822	13.322	2.1378	4.6185	4.4409
256	1.6622	0.7847	13.322	3.2317	37.10	4.4409

Table 1: Error between the solution at different grid points as compared to the exact solution.

We present numerical simulations for Example 2 in Fig. 2 and 3 where we also show the convergence of the two schemes by performing several computations for different grid points. To highlight the efficiency of the derived scheme, we also present simulations based on the CFV scheme, NSFD and NCFV schemes. In Fig. 2(b) and Fig. 3 respectively, one can clearly see the computational power of the nonstandard finite volume scheme and the non-classical finite volume scheme, in these two schemes we do not need the requirement of "at least 10 grid nodes per oscillation" as highlighted in [3]. We also highlight the better performance of NSFV scheme when exact schemes for the boundary conditions are used, see Figs. 2(c) and 2(d). Though the schemes converge to the same solution, it requires around 50 grid nodes to get a stable solution with the classical finite volume scheme, see Fig. 2(a). This is in agreement with the well-known fact that the good performance of nonstandard schemes occurs irrespective of the value of the step size $h = 1/m$, (cf. [2]).

The maximum error calculations are given in Table 2. In the absence of the exact solution, the errors were calculated by comparing the computed solution on a certain number of grids with a reference solution computed on 1024 grid nodes. The efficiency of the derived schemes is evident. The NSFV and the NCFV schemes converge uniformly to the reference solution while there are problems with the CFV scheme for fewer grid points. In particular, we observed the same accuracy between CFV and NSFV with the later using less than 12% and 40% of the grid cells for $\varepsilon = 0.02$

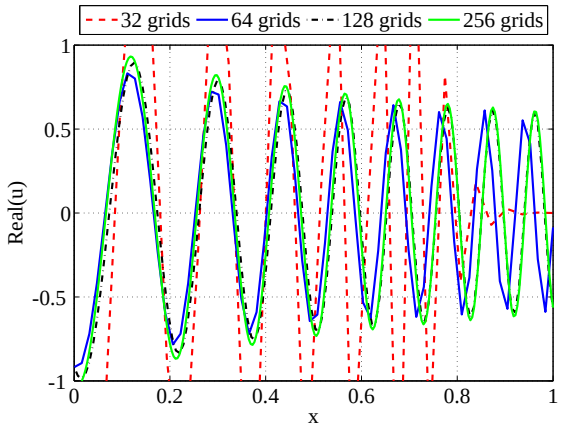

(a) CFV scheme (3.4) with (3.7) and (3.8).

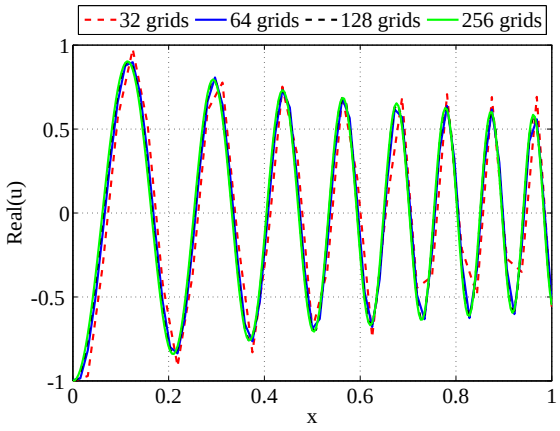

(b) NSFD scheme (4.4) with (6.4) and (6.5).

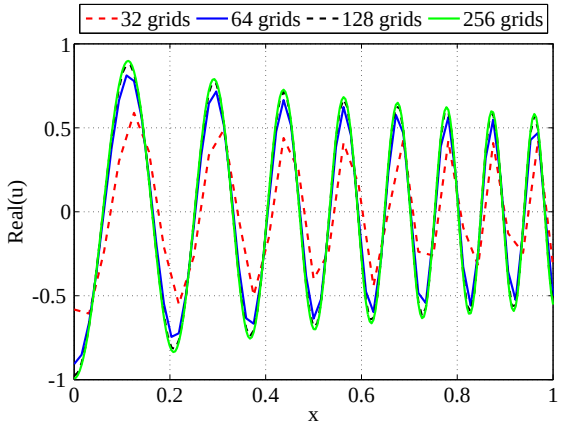

(c) NSFV scheme (6.1) with (3.7) and (3.8).

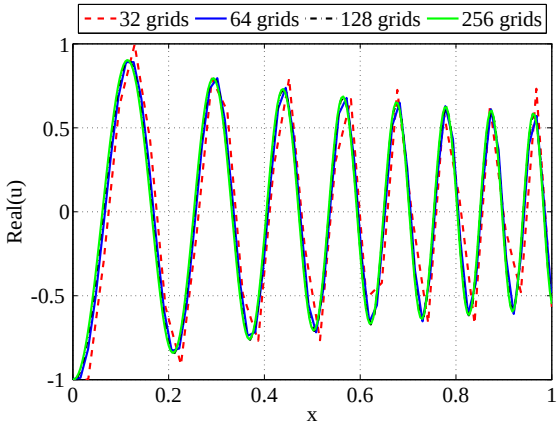

(d) NSFV scheme (6.1) with (6.4) and (6.5)

Figure 2: Convergence of the different schemes for several grid choices with $\varepsilon = 0.02$.

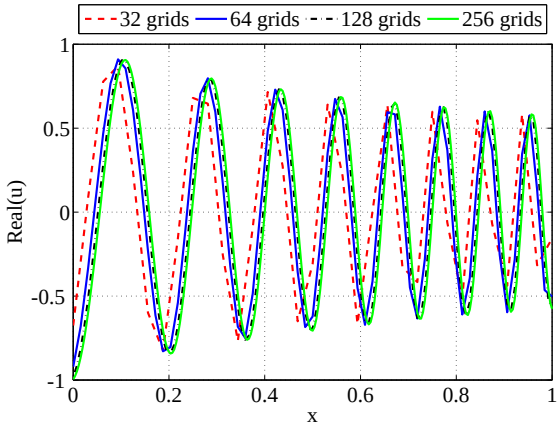

Figure 3: Convergence of the NCFV scheme for several grid choices with $\varepsilon = 0.02$.

and $\varepsilon = 0.002$ respectively, see Table 2.

Grid points	L_∞ Norm error							
	$\varepsilon = 0.02$				$\varepsilon = 0.002$			
	CFV	NSFV	NSFD	NCFV	CFV	NSFV	NSFD	NCFV
32	1.6916	0.1454	0.1401	0.0070	1.1439	2.6162	2.9044	0.0057
64	0.3116	0.0206	0.0203	0.0031	1.1437	2.0825	2.2826	0.0030
128	0.1532	0.0047	0.0047	0.0015	1.0914	4.8390	4.7830	0.0015
256	0.0751	0.0009	0.0010	0.0008	2.8827	0.5704	0.5688	0.0007
512	0.0186	0.0002	0.0006	0.0004	0.6379	0.0232	0.0234	0.0004

Table 2: Error between the solution at different grid points compared with a reference solution at 1024 grid points.

Example 3 *Consider*

$$\begin{cases} -\varepsilon^2 u''(x) - q(x)u(x) = 0, \;\; x \in (0,1), \\ \varepsilon u'(0) + ip(0)u(0) = 2ip(0), \\ \varepsilon u'(1) - ip(1)u(1) = 0, \end{cases} \tag{7.3}$$

with a discontinuous potential

$$q(x) = \begin{cases} 2, & if \;\; 0 \leq x < 0.5, \\ 1, & if \;\; 0.5 \leq x \leq 1.0. \end{cases}$$

The discontinuous potential function is of practical interest (see for example [5, 11]) in resonant tunneling diodes and many other industrial applications.

Example 3 highlights the advantages of the derived NSFV scheme over its NSFD counterpart (4.4) - (4.6) which does not apply here because of the discontinuity of $q(x)$. In particular, the cell average $\bar{q}_j$ computed using the NSFV scheme is more accurate than the approximation in (4.5) for the NSFD scheme where it applies. Numerical simulations are presented in Fig. 4. The kink in Fig. 4(c) is due to the discontinuity in the potential $q(x)$ and the fact that our WKB solution used as a corrector in the NCFV scheme is only valid for $\varepsilon \ll 1$. However, we can see the better performance of the scheme for $\varepsilon = 0.02$.

8 Discussion and conclusion

It has been documented that for the singularly perturbed Schrödinger equation, standard schemes such as finite difference methods require several grid points to provide an accurate and reliable approximation [3]. Therefore, such methods consume much CPU memory and also computing time will be long. This is due to the need to qualitatively resolve the oscillatory solution. In fact, error estimates for the equation are normally computed only when $h \ll \varepsilon$, see for example [12]. This implies that many grid points are employed as $\varepsilon \to 0$. In this work, we have designed a coupled finite volume and nonstandard finite difference scheme in which the features of the Schrödinger equation that cause difficulties are suitably incorporated. These include the perturbation term, the potential term and the boundary conditions. We show computationally that the resulting scheme is capable of preserving the properties of the solution for any number of grid points.

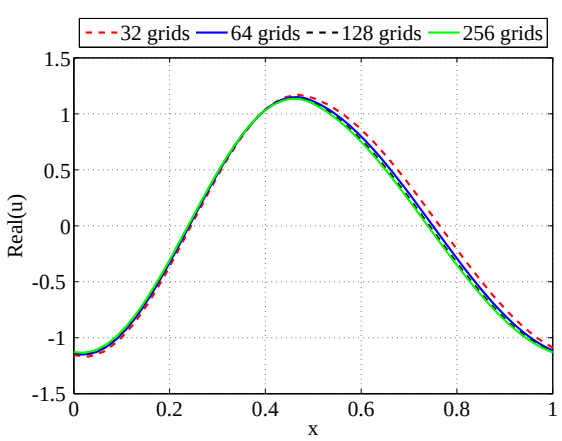

(a) NSFV scheme (6.1) with $\varepsilon = 0.2$

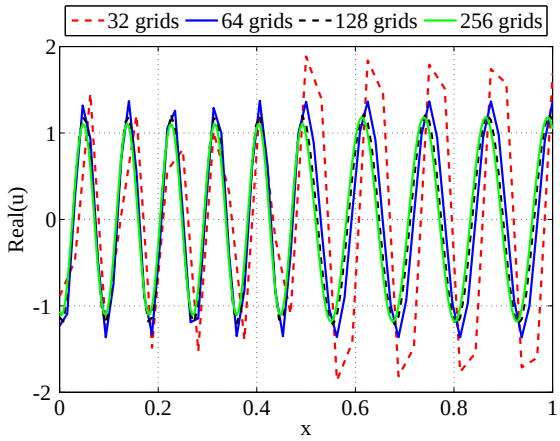

(b) NSFV scheme (6.1) with $\varepsilon = 0.02$

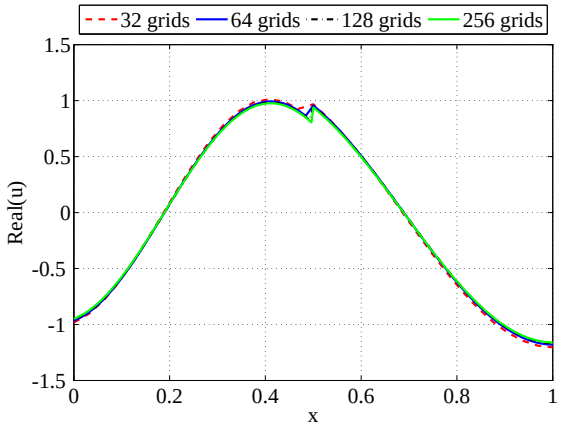

(c) NCFV scheme (5.6) with $\varepsilon = 0.2$

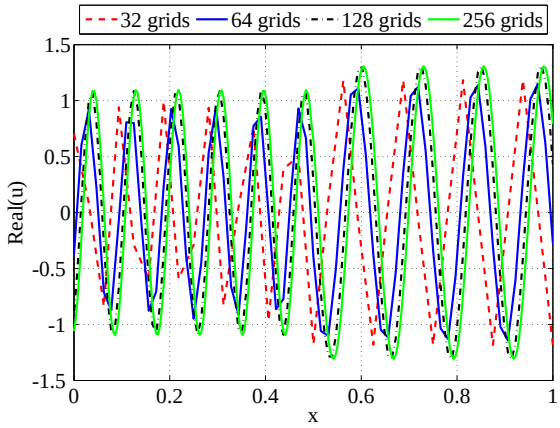

NCFV scheme (6.1) with $\varepsilon = 0.02$

Figure 4: Convergence of the NSFV and NCFV scheme for discontinuous potential function and several grid choices.

The better performance of the designed schemes is evident from the simulations presented in Figs. 1 – 4. We highlight that, for 16 grids points, (simulations not shown here), the classical scheme failed to reproduce the expected oscillatory behavior observed with the NSFV and the NCFV schemes. Tables 1 and 2 support the better performance of the non-standard finite volume scheme as compared to the classical scheme. Note that the choice of ε used here is for illustration only. The same behavior can be extended to other choices of ε. An additional advantage of the proposed schemes is the flexibility to handle cases with discontinuous potential $q(x)$ without the need to careful isolate the location of discontinuities as in adaptive methods. In addition, the superiority of the NSFV scheme with exact schemes for the boundary conditions over the classical ones is evident from the comparison of Fig 2(c) and Fig. 2(d).

This work summarizes our first effort towards designing a robust scheme for the self-consistent Schrödinger-Poisson equation. We plan to extend the method discussed here to design qualitatively stable schemes for Schrödinger-Poisson equation.

Acknowledgements

The authors acknowledge the support of South African NRF and DST/NRF SARChI Chair on Mathematical Models and Methods in Bioengineering and Biosciences (M^3B^2). Thanks are also addressed to the four anonymous reviewers whose suggestions have contributed to the improvement of the paper.

References

[1] J. Alvarez-Ramirez, F.J. Valdes-Parada. Non-standard finite-differences schemes for generalized reaction–diffusion equations. *J. Comput. Appl. Math.*, 228(1), 334-343, 2009.

[2] R. Anguelov and J.M.-S. Lubuma, Contributions to the mathematics of the nonstandard finite difference method and applications, *Numer. Methods PDEs* 17:518-543, 2001.

[3] A. Arnold, N. B. Abdallah, and C. Negulescu. WKB-based schemes for the oscillatory 1D Schrödinger equation in the semiclassical limit. *SIAM J. Numer. Anal.*, 49(4):1436–1460, 2011.

[4] Y. Dumont, J. M-S. Lubuma. Non-standard finite-difference methods for vibro-impact problems. *Proc. R. Soc. A*, 461:1927–1950, 2005.

[5] Wu, Hao. High order scheme for Schrodinger equation with discontinuous potential I: immersed interface method. *Numer. Math. Theor. Meth. Appl.*,4(4), 2011.

[6] Hernandez-Martinez, E., Valdes-Parada, F.J., Alvarez-Ramirez, J. A Green's function formulation of nonlocal finite-difference schemes for reaction–diffusion equations *J. Comput. Appl. Math.*, 235(9):3096–3103, 2011.

[7] M. H. Holmes. *Introduction to perturbation methods.* Springer, 2012.

[8] G. L. Snider, I-H. Tan, and E. L. Hu. Electron states in mesa-etched one-dimensional quantum well wires. *J. Appl. Phys.*, 68(6):2849–2853, 1990.

[9] I-H. Tan, G. L. Snider, L. D. Chang, and E. L. Hu. A self-consistent solution of Schrödinger-Poisson equations using a nonuniform mesh. *J. Appl. Phys.*, 68(8):4071–4076, 1990.

[10] O. Pinaud. Transient simulations of a resonant tunneling diode. *J. Appl. Phys.*, 92(4):1987–1994, 2002.

[11] N. B. Abdallah and O. Pinaud. Multiscale simulation of transport in an open quantum system: Resonances and WKB interpolation. *J. Computat. Phys.*, 213(1):288–310, 2006.

[12] C. Negulescu. Numerical analysis of a multiscale finite element scheme for the resolution of the stationary Schrödinger equation. *Numer. Math.*, 108(4):625–652, 2008.

[13] R. E. Mickens. Novel explicit finite-difference schemes for time-dependent Schrödinger equations. *Comput. Phys. Commun.*, 63(1):203–208, 1991.

[14] R. E. Mickens. *Nonstandard finite difference models of differential equations*. World Scientific, 1994.

[15] R. E. Mickens. *Advances in the Applications of Nonstandard Finite Diffference Schemes*. World Scientific, 2005.

[16] K. C. Patidar and K. K. Sharma. Uniformly convergent non-standard finite difference methods for singularly perturbed differential-difference equations with delay and advance. *Int. J. Numer. Meth. Eng.*, 66(2):272–296, 2006.

[17] J. M-S. Lubuma and K. C. Patidar. Uniformly convergent non-standard finite difference methods for self-adjoint singular perturbation problems. *J. Comput. Appl. Math.*, 191(2):228–238, 2006.

[18] J. M-S. Lubuma and K. C. Patidar. Non-standard methods for singularly perturbed problems possessing oscillatory/layer solutions. *Appl. Math. Comput.*, 187(2):1147–1160, 2007.

[19] R. E Mickens. Nonstandard finite difference schemes for differential equations. *J. Diff. Eq. Appl.*, 8(9):823–847, 2002.

[20] K. C Patidar. On the use of nonstandard finite difference methods. *J. Diff. Eq. Appl.*, 11(8):735–758, 2005.

[21] C-Y Jung and R. Temam. Finite volume approximation of one-dimensional stiff convection-diffusion equations. *J. Sci. Comput.*, 41(3):384–410, 2009.

[22] C-Y. Jung and T. B. Nguyen. Semi-analytical numerical methods for convection-dominated problems with turning points. *Int. J. Numer. Anal. Model.*, 10(2):314–332, 2013.